JOURNAL OF VIROLOGY, July 2008, p. 7078–7088 Vol. 82, No. 14
0022-538X/08/$08.00+0 doi:10.1128/JVI.00619-08

The Immune Response to Herpes Simplex Virus Type 1 Infection in Susceptible Mice Is a Major Cause of Central Nervous System Pathology Resulting in Fatal Encephalitis▽†

Patric Lundberg,[1,2]‡ Chandran Ramakrishna,[1] Jeffrey Brown,[4] J. Michael Tyszka,[5] Mark Hamamura,[6] David R. Hinton,[7] Susan Kovats,[8] Orhan Nalcioglu,[6] Kenneth Weinberg,[4] Harry Openshaw,[3] and Edouard M. Cantin[1,2,3]*

Divisions of Virology,[1] Immunology,[2] and Neurology,[3] Beckman Research Institute and City of Hope National Medical Center, Duarte, California 91010; Department of Pediatrics, Children's Hospital Los Angeles, Los Angeles, California 90033[4]; Division of Biology, California Institute of Technology, Pasadena, California 91125[5]; Center for Functional Onco-Imaging, University of California, Irvine, California 92697[6]; Department of Pathology, Keck School of Medicine, Beckman Macular Research Center, University of Southern California, Los Angeles, California 90033[7]; and Arthritis and Immunology Research Program, Oklahoma Medical Research Foundation, Oklahoma City, Oklahoma 73104[8]

Received 19 March 2008/Accepted 6 May 2008

This study was undertaken to investigate possible immune mechanisms in fatal herpes simplex virus type 1 (HSV-1) encephalitis (HSE) after HSV-1 corneal inoculation. Susceptible 129S6 (129) but not resistant C57BL/6 (B6) mice developed intense focal inflammatory brain stem lesions of primarily F4/80$^+$ macrophages and Gr-1$^+$ neutrophils detectable by magnetic resonance imaging as early as day 6 postinfection (p.i.). Depletion of macrophages and neutrophils significantly enhanced the survival of infected 129 mice. Immunodeficient B6 (IL-7R$^{-/-}$ Kit$^{w41/w41}$) mice lacking adaptive cells (B6-E mice) and transplanted with 129 bone marrow showed significantly accelerated fatal HSE compared to B6-E mice transplanted with B6 marrow or control nontransplanted B6-E mice. In contrast, there was no difference in ocular viral shedding in B6-E mice transplanted with 129 or B6 bone marrow. Acyclovir treatment of 129 mice beginning on day 4 p.i. (24 h after HSV-1 first reaches the brain stem) reduced nervous system viral titers to undetectable levels but did not alter brain stem inflammation or mortality. We conclude that fatal HSE in 129 mice results from widespread damage in the brain stem caused by destructive inflammatory responses initiated early in infection by massive infiltration of innate cells.

Herpes simplex virus type 1 (HSV-1) infections are widespread in developed countries, with estimates of seropositivity exceeding 50% (54). Primary infections in immunocompetent individuals are usually mild or even asymptomatic and result in lifelong latent infections in sensory ganglia and the central nervous system (CNS) (5). Reactivated HSV-1 can result in recurrent diseases of mucous membranes (e.g., gingivostomatitis and herpes labialis) and herpes keratitis, an immunopathological disease that is a leading cause of blindness (39). Also, HSV-1 is the most common cause of fatal, sporadic encephalitis in immunocompetent individuals (40, 56). Improvements in diagnosis and antiviral drug treatment have dramatically reduced the morbidity and mortality of HSV-1 encephalitis (HSE) (55), although some patients fail to respond or subsequently suffer neurological relapses after completing a standard treatment course (18, 55).

Clinical and animal model studies have clearly demonstrated the importance of genetic makeup in resistance to a broad range of infectious agents (15, 41). In regard to HSV-1, C57BL/6 (B6) and related B10 mouse strains are resistant, while other strains, such A/J, BALB/c, 129S6 (129), and DBA/2J, are susceptible to fatal infections (21, 23, 25). In these animal models, mortality results from CNS infection. In prior studies, we defined the herpes resistance locus (*Hrl*) on mouse chromosome 6 as a major determinant of resistance (22, 25); however, ongoing studies indicate that resistance to HSE is genetically very complex, involving multiple interacting loci, with tumor necrosis factor playing a critical role (26) (unpublished results).

The mechanism by which HSV-1 CNS infection causes death has not been defined. Counterintuitively, necropsy virus titers of nervous system tissues do not correlate with mouse resistance or susceptibility genotype (25, 26). These and other observations have led to the suggestion that variation of the host inflammatory response may play a major role in determining HSV fatality. Intense inflammatory responses in CNS tissues in a mouse model of HSE have been reported, with tumor necrosis factor and macrophage chemoattractant protein 1 being expressed prominently (43). Also, in vitro and in vivo studies have shown that human and mouse microglia nonproductively infected with HSV-1 express a variety of proinflammatory cytokines and chemokines, consistent with their involvement in

* Corresponding author. Mailing address: Beckman Research Institute, City of Hope National Medical Center, 1500 E. Duarte Road, Duarte, CA 91010. Phone: (626) 301-8480. Fax: (626) 301-8457. E-mail: ecantin@coh.org.

† Supplemental material for this article may be found at http://jvi.asm.org/.

‡ Present Address: Department of Microbiology, Eastern Virginia Medical School, Norfolk, VA.

▽ Published ahead of print on 14 May 2008.

early innate responses against invading virus (19, 20). Whether such innate inflammatory responses are protective or deleterious has not yet been clarified.

We present here a series of studies comparing HSE in susceptible 129 mice and resistant B6 mice. These studies support the hypothesis that the immune response is the major cause of CNS pathology resulting in a fatal course and that hyperinflammatory responses initiated by early infiltrating innate cells play a key role in the development of this pathology. Our results have important implications for understanding the pathogenesis and clinical treatment of HSE.

MATERIALS AND METHODS

Mouse strains, HSV infection, and monitoring. The B6 empty strain (B6-E; *IL-7R*$^{-/-}$ *Kit*$^{w41/w41}$) was derived by backcrossing the B6.IL-7R$^{-/-}$ strain (B6.129S7-Il7^{rtm1Imx}/J) to the B6.Kit$^{w41/w41}$ mutant strain (C57BL/6J-Kit^{W-41J}); mice homozygous for both mutations were selected after 10 backcrosses (N10). Both parental strains were obtained from the Jackson Laboratories (Bar Harbor, ME), as were C57BL/6J mice. 129S6 mice were obtained from Taconic (Germantown, NY) or bred in-house. Mice used in experiments were 6 to 10 weeks of age or older (for bone marrow transplantation [BMT] studies). Master stocks of HSV-1 strain 17^{+} composed of only of cell-released virus were prepared in and their titers determined on mycoplasma-free CV-1 cell monolayers. Single-use aliquots of virus in Hanks balanced salt solution supplemented with 2% fetal bovine serum were stored at −80°C. Mice were inoculated as previously described with HSV by corneal scarification with 3.2×10^3 PFU HSV-1 17^{+}, which is a 10× 50% lethal dose for 129S6 mice (25). HSV replication was monitored as shedding of HSV-1 in the tear film, as previously described (25). Acyclovir (ACV) at 50 mg/kg of body weight (or a phosphate-buffered-saline [PBS] control) was administered by intraperitoneal (i.p.) injection. The City of Hope Institutional Animal Care and Use Committee approved of all animal procedures, which additionally were in compliance with the Guide for the Care and Use of Laboratory Animals.

Isolation of mononuclear cells from BS of HSV-1-infected mice. We adapted the method described by Ford et al. (8). Briefly, two or three pooled brain stems (BS) were minced and digested with collagenase, after which the cell suspension was centrifuged through a two-step Percoll gradient. The resulting enriched population of viable mononuclear cells included lymphocytes as well as microglias identified as CD45^{Int} CD11b^{+} F4/80^{+} and CNS macrophages characterized as CD45^{Hi} CD11b^{+} F4/80^{+}; the latter two populations are morphologically and functionally distinct (8, 14). Cells isolated using this procedure retained high viability even after further purification by cell sorting, provided that GKN/BSA buffer was used (8). Mononuclear cell yields from a normal brain range from 0.8×10^5 to 2×10^5 with no T cells present (14), but higher cell yields are found for inflamed trigeminal ganglia and BS of HSV-inoculated mice. Cell viability is usually greater than 95%; control digestions of spleen and draining lymph node (dLN) cells with collagenase indicated that the enzyme had no effect on the expression of cell surface markers or the functionality of CD4^{+} and CD8^{+} T cells (33).

Flow cytometry. Analysis of surface marker expression was done by staining splenocytes or mononuclear cells isolated from the BS of HSV-1-infected mice with fluorochrome-conjugated antibodies. Spleens were mechanically disrupted using sterile glass slides, and erythrocytes were lysed using hypotonic buffer. A conventional sandwich enzyme-linked immunosorbent assay was used to determine the presence of cytokines. A list of antibodies used is provided in the supplemental material.

MRI on live HSV-1-infected mice. Magnetic resonance imaging (MRI) was performed at the Biological Imaging Resource Center at the California Institute of Technology or at the Center for Functional Onco-Imaging, University of California Irvine. Parameters for MRI are provided in the supplemental material.

In vivo depletion of neutrophils and macrophages. To deplete neutrophils, mice were treated with protein G-purified anti-Gr-1 monoclonal antibody (MAb) (RB6-8C5) that binds Ly-6G/C, present on neutrophils (7). The RB6-8C5 hybridoma was provided by Daniel Berg (University of Iowa) with the permission of Robert Coffman (formerly of DNAX) (11), and MAb was purified from culture supernatants by using protein G columns (HiTrap, Amersham Pharmacia). Each mouse was given 500 μg Gr-1 MAb or rat isotype control antibody by i.p. injection on days −1, 0, 2, 4, 6, and 8 postinfection (p.i.). The neutrophils were characterized as CD11b^{+} Ly-6G^{hi} (57); hence, their depletion was monitored by staining spleen cells from two mice sacrificed on day 8 p.i. with antibodies to CD11b and Ly-6G; these mice were not given anti-Ly-6G/C MAb on day 8 p.i. (see Fig. S1A and B in the supplemental material). Procedures and analysis of Gr-1 MAb cross-reactivity are provided in the supplemental material.

Macrophages were depleted in vivo by treating mice with liposome-encapsulated dichloromethylene biphosphonate (clodronate) on days 0, 2, 4, 6, and 8 p.i.; each mouse received 200 μl clodronate by i.p. injection. Mice were inoculated with HSV-1 on day 0 and immediately injected with clodronate. Control mice were injected with PBS alone, as recommended by the supplier (51). The extent of macrophage depletion was monitored by flow cytometry of pooled peritoneal exudate cells stained for CD11b and F4/80. Peritoneal exudate cells were obtained from two mice sacrificed on day 8 p.i. that had last received clodronate on day 6; Fig. S1M and N in the supplemental material show >95% depletion of CD11b^{+} cells in this analysis.

Histology and immunostaining. Anesthetized mice were sacrificed by cardiac perfusion of PBS at room temperature. BS were either (i) snap frozen in liquid nitrogen-cooled isopentane, embedded in OCT embedding matrix, and cut in 6-μm sections or (ii) perfused with cold 4% paraformaldehyde, incubated overnight in 4% paraformaldehyde, embedded in paraffin, and cut in 100-μm step sections, with multiple 6-μm serial sections collected at each step. For paraffin sections, the first section from each step was stained with hematoxylin and eosin (H&E) and serial adjacent sections from the most affected steps were stained for the presence of Gr-1^{+} neutrophils, F4/80^{+} macrophages (MAb clone A3-1), CD4^{+} (MAb clone GK1.5) and CD8^{+} (MAb clone 53-6.72) T cells, and HSV antigen (rabbit polyclonal DAKO; Glostrup, Denmark) by using standard immunohistochemistry (Vector ABC Elite; AEC chromogen). Spleen sections were used as positive controls, and primary antibodies were omitted for negative controls.

BMT. B6-E mice (B6.IL-7R$^{-/-}$ *Kit*$^{w41/w41}$) were used as recipients for BMT. The dominant-negative *Kit*$^{w41/w41}$ mutation affects primarily the kinase but not other aspects of the c-Kit receptor (34). The B6-E mouse lacks αβ T, mature B (CD19^{+} early pro-B cells are present as expected) (10, 53) (see Fig. S2A in the supplemental material), and γδ T cells as a result of interleukin 7R deficiency and the *Kit*$^{w41/w41}$ mutation (9, 13, 31, 37), but monocyte subsets, NK cells (see Fig. S2A in the supplemental material), and dendritic cells (see Fig. S2B and C in the supplemental material) were present at levels comparable to those of B6. Kit mutations additionally interfere with mast cell development and function, and B6-E mice, like *Kit*$^{W/W-v}$ mice, are deficient in tissue mast cells (17, 28, 38).

Six-week-old B6-E mice, either irradiated with 650 rads or nonirradiated, were reconstituted with 129 or B6 bone marrow. Retro-orbital bleeds at about 10 weeks posttransplantation were analyzed for B (CD19) and T (Thy1.2) cells to validate engraftment (not shown). In irradiated mice, roughly 70% of the macrophages and all of the B and T cells are donor derived. At about 12 weeks, the different mouse groups were blind challenged with HSV-1. Although B6 and 129 mice are histocompatible, they differ at minor major histocompatibility complex (MHC) loci; hence, it was important to exclude the possibility of development of graft-versus-host disease (GVHD) for cross-strain BMTs. Examination of liver and small intestine tissue H&E sections obtained from four or five normally engrafted mice in each transplant group failed to reveal morphological changes typical of GVHD (not shown); the pathology report stated that all tissue sections appeared morphologically normal, which excludes GVHD as a confounding factor in the transplant experiments.

Statistical analysis. Mortality data were analyzed by log-rank testing (taking into account both time of death and final mortality). Titers and cytokine production (averages ± standard errors of the means) were analyzed using the two-tailed Student *t* test or the Mann-Whitney test where appropriate and judged significant when P was <0.05. Flow cytometry data were judged to be different based on mean channel changes between replicate test and control samples or >2-fold changes in relative or absolute numbers of cells as appropriately applicable.

RESULTS

Visualization of BS inflammation by MRI and immunohistopathology in susceptible 129 and resistant B6 mice. To compare BS infection, B6 or 129 mice were inoculated with HSV by corneal scarification and representative mice were anesthetized for an MRI scan at day 6 p.i. Increased signals on T2-weighted sequences corresponding to the trigeminal root entry zone and nuclei were seen in 129 but not in B6 mice (Fig. 1A and B). To confirm that this increased signal (reflecting the

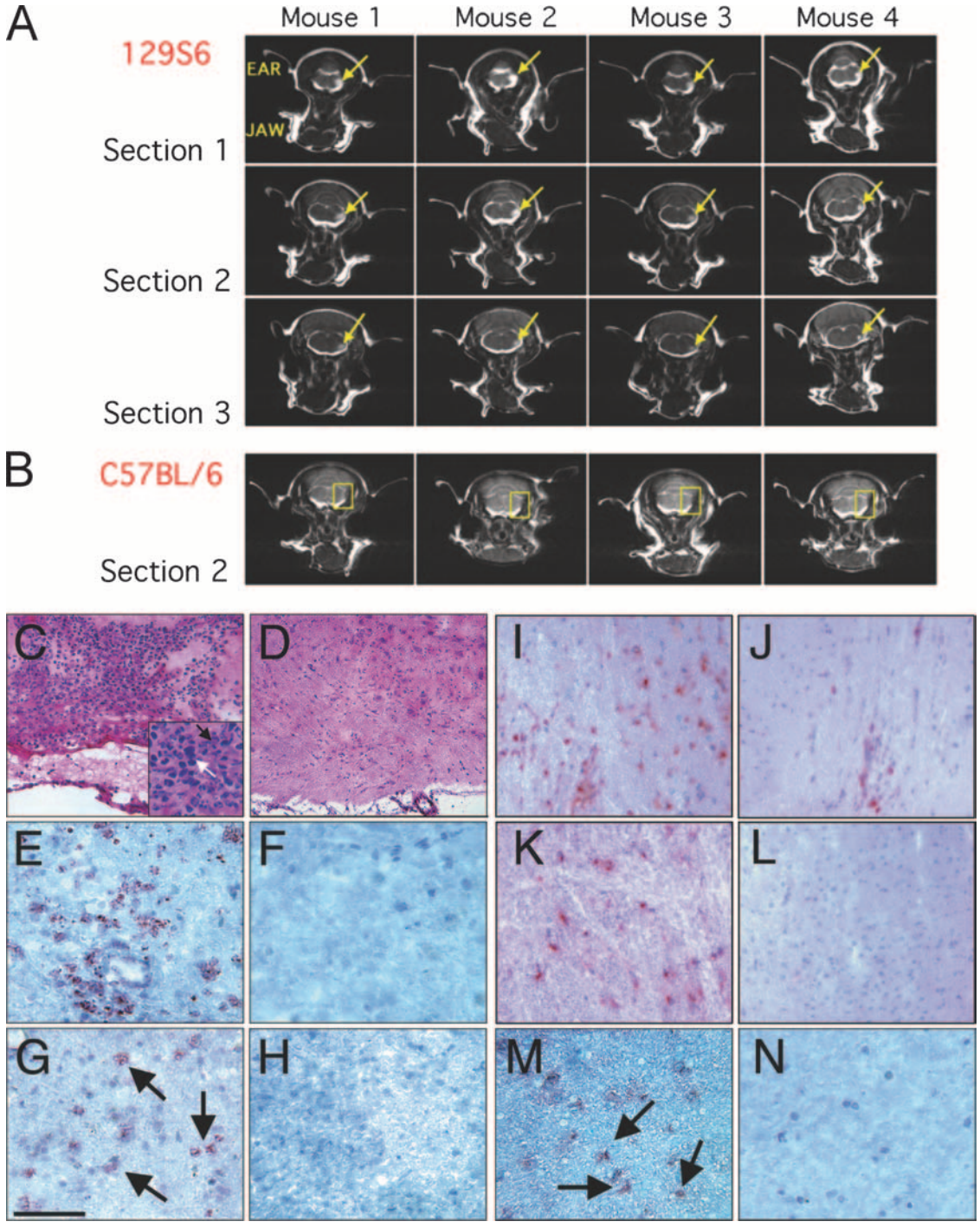

FIG. 1. Visualization of BS lesions by MRI and histology from HSV-infected 129 and B6 mice. (A and B) Coronal T2-weighted MRIs at the level of the trigeminal nerve root in four 129 mice (A) (three consecutive MRI sections, with arrows indicating increased signals in trigeminal nuclei) and four B6 mice (B) (corresponding to section 2 in panel A, with rectangles outlining the areas of the trigeminal nuclei not showing increased signals) at day 6 p.i. Data shown are representative of two experiments. (C and D) H&E-stained, frozen BS sections from an infected 129 mouse (C) (with an extensive inflammatory infiltrate [shown at a higher magnification in the inset] composed of neutrophils [black arrow] and mononuclear cells [white arrow]) and a B6 mouse (D) (the corresponding section with scant inflammatory cells) at day 7 p.i. (E to M) BS immunohistochemical staining at day 7 p.i. of 129 mice positive for perivascular F4/80$^+$ macrophages (E), Gr-1$^+$ neutrophils (G), CD4$^+$ T cells (I), CD8$^+$ T cells (K), and HSV antigen (M), with corresponding negative immunochemical staining in B6 mice (F, H, L, M), except for an occasional perivascular T cell, as shown in panel J. The bar shown in panel G is 75 μm.

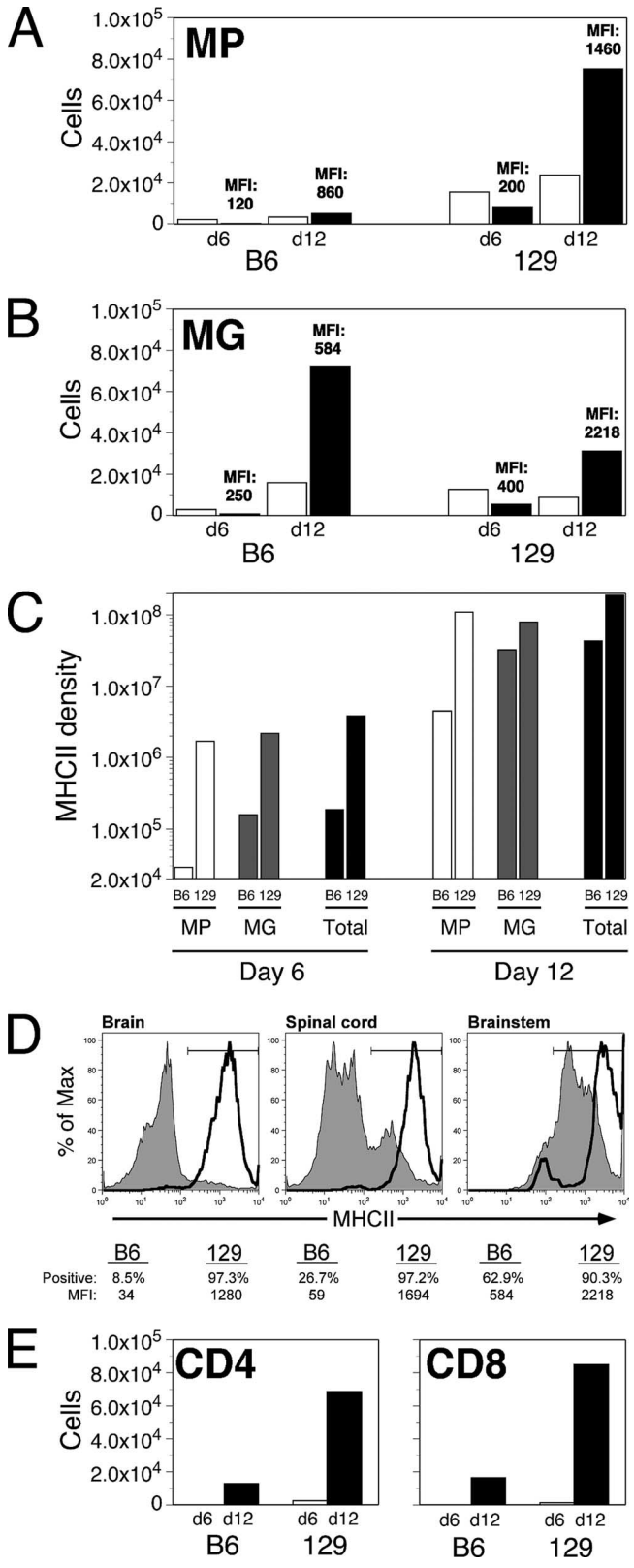

FIG. 2. Accumulation and activation of immune cells over time in BS of susceptible and resistant mice. Cells were isolated from infected BS of B6 and 129 mice on day 6 or day 12 p.i. and analyzed for surface marker expression. (A) Macrophages (MP; $CD11b^+$ $F4/80^+$ $CD45^{hi}$). (B) Microglia (MG; $F4/80^{low}$ $CD45^{int}$). (C) Bar graphs indicate the absolute cell numbers of MHC-II-negative (open bars) and -positive (filled bars) macrophages recovered from pooled BS ($n = 3$). MFI is indicated for the MHC-II^+ gates. Bar graphs of total MHC-II density on macrophages (white bars), microglia (gray bars), and MP plus MG (Total; black bars) in the BS of B6 (left) and 129 (right) mice on days 6 and 12 are shown. MHC-II density was calculated by multiplying the absolute number of MHC-II^+ cells by their MFIs, as indicated in panels A and B, and provides a measure of the relative number of MHC molecules in the BS. (D) MHC-II expression on MG in three different CNS compartments of B6 (filled gray histograms) and 129 (open thick line) mice on day 12. The MFI is also indicated for each strain. MG were gated as viable forward scatter-side scatter and side scatter-$CD45^{int}$ events, and data represent typical population profiles from pooled tissues of two to four mice and are representative of two experiments. The MHC-II^+ gate is shown for each histogram overlay, and the percentage of positive cells for each strain and tissue is given below each panel. (E) Absolute numbers of $CD4^+$ $CD45^{hi}$ (left panel) or $CD8^+$ $CD45^{hi}$ (right panel) T-cells in BS from B6 and 129 mice on days 6 (open bars) and 12 (filled bars).

focal edema) (Fig. 1A) was secondary to inflammation, cryosections were prepared from 129 and B6 mice on day 7 p.i. for H&E and immunostaining. BS sections from 129 animals showed multifocal areas of meningoencephalitis, consistent with the MRI. In some areas, the inflammatory infiltrate was associated with fibrinoid vasculitis (not shown) and necrosis of associated BS parenchyma (Fig. 1C and D). On H&E sections, the infiltrate was mixed (Fig. 1C); however, neutrophils appeared to predominate. In contrast, BS sections from B6 animals were for the most part normal, with only rare inflammatory cells within the subarachnoid space or parenchyma and no areas of necrosis (Fig. 1D). Immunohistochemical staining of 129 sections showed extensive infiltration of the tissue with macrophages (panel E) and neutrophils (Fig. 1G). Scattered $CD4^+$ and $CD8^+$ cells were seen infiltrating intact tissues adjacent to more-inflamed necrotic regions (Fig. 1I and K). Staining for HSV antigens revealed numerous immunoreactive cells (Fig. 1M), including neurons, but the antigen-positive cells did not appear localized to areas of inflammation. Macrophages were absent in B6 BS sections (Fig. 1F) except for focal areas in which a mild increase in macrophages was seen in the subarachnoid space (not shown). There were no neutrophils or $CD8^+$ T-cell infiltrates (Fig. 1H and L); however, occasional perivascular $CD4^+$ cells were noted (Fig. 1J). HSV antigen staining was negative (Fig. 1N). Remarkably, HSV-1 was cleared from the BS of wild-type B6 mice in the virtual absence of inflammatory responses detectable by either MRI or histology at days 6 and 7 p.i. In contrast, the massive tissue destruction observed in the BS of 129 mice was associated with a dramatic influx of predominantly neutrophils and macrophages and the persistence of HSV-1 antigen.

Analysis of isolated BS immune cells early in HSV-1 infection of susceptible 129 and resistant B6 mice. To further determine differences in inflammatory responses in B6 and 129 mice, infiltrating BS $CD45^+$ mononuclear cells were analyzed by flow cytometry. Macrophages comprised over 75% of infiltrating cells in both strains at day 6 p.i., and there were ~4-fold increases in the macrophage compartment in both strains by day 12 p.i. As shown in Fig. 2A, there were 9- to 10-fold more macrophages present in 129 mice at both day 6 and day 12 p.i. Activated macrophages, as indicated by MHC class II (MHC-

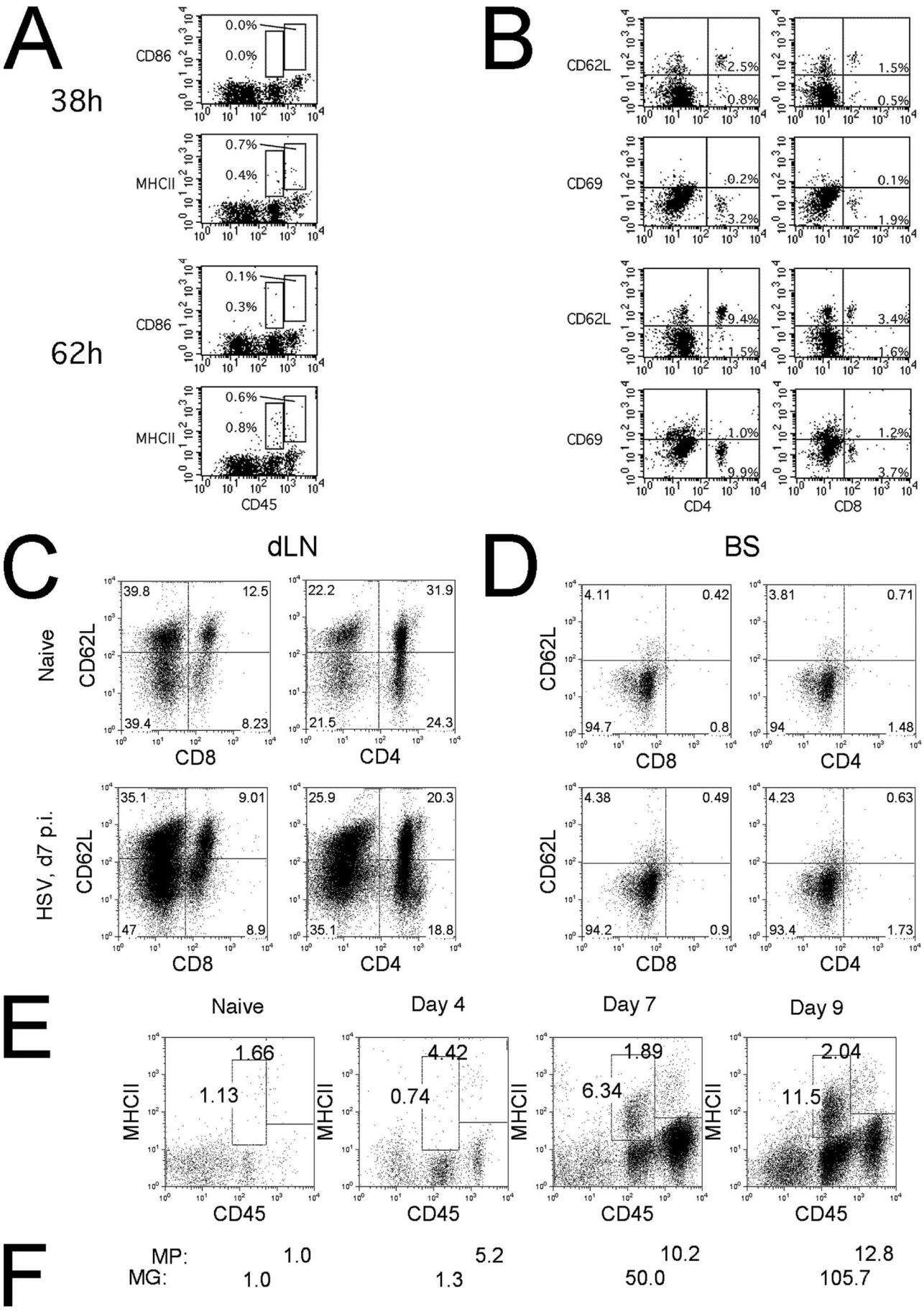

II) expression (Fig. 2A) were 58-fold greater in 129 mice at day 6 and 24-fold greater at day 12 p.i. (Fig. 2C). Although more microglial cells were isolated from B6 BS (Fig. 2B), 129 microglia expressed 13.7-fold-higher levels of MHC-II at day 6 p.i., as indicated by MHC-II density (Fig. 2C), reflecting a more activated state. Only a few $CD4^+$ and $CD8^+$ T cells were present in 129 BS at day 6 p.i., while T cells were not present in B6 BS. By day 12 p.i., T cells were seen in the BS of both mouse strains; however, their numbers were three- to fourfold greater in 129 BS (Fig. 2E). These differences in T-cell accumulation and MHC-II expression in the BS reflect the overall greater inflammatory response in 129 than in B6 mice.

To investigate whether the microglial activation in 129 CNS extended beyond the BS, cells were isolated from whole brain and spinal cord on day 12 p.i. and analyzed by flow cytometry for MHC-II expression. Figure 2D shows significantly higher activation of $CD45^{int}$ $F4/80^+$ microglia in all three CNS compartments in 129 than in B6 mice, as judged by MHC-II expression. Differences in MHC-II expression were most pronounced in brain and spinal cord. More than 97% of microglia were MHC-II positive ($MHC\text{-}II^+$), with a mean fluorescence intensity (MFI) above 1,200 in 129 mice, while fewer than 30% of B6 microglia were $MHC\text{-}II^+$, with an MFI less than 100 (Fig. 2D).

Next, we focused on early innate responses in 129 mice to identify the cell types underlying development of inflammatory lesions in the BS. From 38 h to 9 days p.i., the number of activated $CD11b^+$ $F4/80^+$ monocytes expressing MHC-II increased steadily (Fig. 3A and E). Separation of the $CD11b^+$ $F4/80^+$ population based on CD45 expression revealed that increased MHC-II expression was due primarily to activation of microglia ($CD11b^+$ $F4/80^+$ $CD45^{Int}$) and, to a lesser extent, macrophage ($CD11b^+$ $F4/80^+$ $CD45^{Hi}$) infiltration (Fig. 3A and E). Although, as percentages of total mononuclear cells, macrophage numbers did not change markedly, their absolute numbers increased from 62 h through day 9 p.i. as much as 13-fold (Fig. 3F shows change relative to cells from naïve mice below each panel in Fig. 3E). Marked activation of microglia occurred between day 4 and day 7 p.i. (50-fold) and was sustained through day 9 (100-fold), as evidenced by upregulation of MHC-II expression (Fig. 3E).

Mononuclear cells infiltrating the BS of mock- or HSV-1-infected mice at day 7 p.i. were stained for CD4 or CD8 and CD62L to determine their activation statuses in comparison to those of $CD4^+$ and $CD8^+$ T cells isolated from the dLN. As expected, there were significantly more cells in the dLNs of infected mice than in those of mock-infected mice, 5×10^7 and 1.75×10^6 cells per mouse, respectively. Activated $CD4^+$ and $CD8^+$ T cells displaying a highly activated phenotype ($CD62L^{low}$) were four- to fivefold more numerous in infected than in uninfected dLNs (Fig. 3C). Although approximately twice as many mononuclear cells infiltrated the BS of infected mice compared to those of mock-infected mice at day 7 p.i. (1.85×10^5 events per infected BS compared to 1.02×10^5 events per mock-infected BS), $CD4^+$ and $CD8^+$ T cells were largely absent (Fig. 3D). However, by day 13 p.i. the BS contained significant numbers of activated $CD4^+$ and $CD8^+$ T cells (18.0% and 14.9%, respectively, of the infiltrating mononuclear cell population; not shown). Thus, although activated T cells are plentiful in the dLN at day 7 p.i., their accumulation in the infected BS is delayed until after day 8 p.i., as we previously reported (4).

TABLE 1. Mouse strain differences in TLR expression[a]

Target	B6 ΔC_T[b]	129 ΔC_T	Difference ($2^{\Delta\Delta t}$)[c]
muTLR2	8.7	8.4	No difference
muTLR3	ND	ND	ND
muTLR4	4.8	4.4	No difference
muTLR6	32.9	24.0	129 level is 480× higher
muTLR7	12.3	12.6	No difference
muTLR9	3.6	2.5	129 level is 2.2× higher

[a] cDNA from PEC-derived RNA from naive wild-type mice was used as a template for Sybr green PCR amplification, using primers for the target murine TLR (muTLR) indicated. Data were combined from four experiments. ND, not done.
[b] ΔC_T is calculated as net C_T difference relative to GAPDH level.
[c] $2^{\Delta\Delta t}$ is calculated as the ΔC_T difference between B6 and 129.

Differences in cellular CNS infiltration between 129 and B6 mice during acute infection could relate to differences in sensing HSV-1 infection. We examined the expression levels of selected Toll-like receptors (TLRs) on peritoneal exudate macrophages because in vivo depletion during infection confirmed their involvement in pathogenesis of HSE (26). As determined by real-time PCR, expression of TLR9 was 2.2-fold higher in 129 than in B6 macrophages (Table 1). Although TLR2, -4, and -7 were expressed at equivalent levels, TLR6, which is known to cooperate with TLR2 for recognition of lipopeptides, was expressed at markedly higher levels on 129 (480-fold higher) than on B6 peritoneal exudate macrophages (Table 1).

Depletion of neutrophils or macrophages during HSV-1 infection increases survival of 129 mice. To determine the protective effect of neutrophils or macrophages on mortality, cell depletion studies were done with administration of anti-Gr-1 MAb or clodronate, respectively, to HSV-1-inoculated 129 mice. As shown in Fig. 4, median survival times were 4 to 5 days longer for depleted mice ($P = 0.007$ for neutrophil depletion and $P = 0.012$ for macrophage depletion). 129 mice depleted of both neutrophils and macrophages did not show any additional survival advantage, and by day 11, there was no difference in mortality between any of the treatment groups and the mock-treated controls, probably due to the rapid reappearance of neutrophils, as noted in earlier studies (1, 46,

FIG. 3. Infiltrating cells in the BS of HSV-infected 129 mice and activation of microglia. Cells isolated from BS of HSV-infected 129 mice at 38 h and 62 h p.i. were stained for CD45 (A) and CD4 and CD8 (B) surface markers and activation molecules (MHC-II or CD86 [A] and CD62L or CD69 [B]). Increases in numbers and activation (loss of CD62L) of CD4 and CD8 T cells in dLNs on day 7 (C) were not seen for CD4 and CD8 T cells retrieved from BS of the same mice (D). BS cells stained for CD45 and MHC-II showed a continued increase in activation of microglia ($CD45^{int}$) until day 9 p.i. (with peaks at 11.5% of the total). (E) Absolute increases in macrophages (MP) and microglias (MG) relative to levels for naïve mice (day 0) are indicated below panel E for days 4 to 9 p.i. (F) Data shown are representative of three experiments for panels A and B and two experiments for panels C, D, and E.

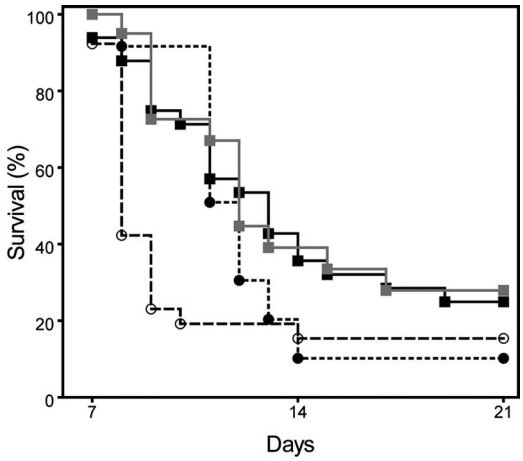

FIG. 4. Depletion of neutrophils or macrophages during acute HSV infection enhances survival. Compared to mock treatment of 129 mice (open circles, dashed line, PBS or rat immunoglobulin G), Gr-1 MAb (black squares), clodronate (gray squares), and combination treatment with both Gr-1 MAb and clodronate (black circles) significantly delayed mortality (the mean survival time was prolonged to day 12 or 13, versus day 8 for controls). Survival on day 10 was highly significant for all treatment groups ($P < 0.003$ for each pairwise comparison to 129 mock controls). Data shown are combined from five different experiments. The overall statistical differences at the end of the experiments were as indicated: **, $P < 0.005$; *, $P < 0.05$ for comparison to the MOCK group; ns, not significantly different.

48) and shown here by the tendency for rapid reappearance of Gr-1$^+$ cells (see Fig. S1A and B in the supplemental material). The timings of repopulation of the spleen by different macrophage subsets are variable after clodronate treatment (6, 32).

Transfer of resistance or susceptibility to fatal HSE by BMT: effect on BS MRI, histopathology, and HSV-1 tear film shedding. Prolongation of survival by cell depletion in susceptible 129 mice (Fig. 4) suggests the possibility that mouse strain differences in resistance to HSE may at least in part be encoded in hematopoietic cells. To investigate this possibility, we transplanted bone marrow from H-2^b MHC-histocompatible donor 129 or B6 mice into immunodeficient B6 empty recipient mice (B6-E), which were gamma irradiated or nonirradiated. Regardless of irradiation status, all B6-E mice receiving B6 bone marrow survived (results for these two groups are combined in Fig. 5). In contrast, there was significant mortality with 129 BMTs in both nonirradiated B6-E recipients ($P < 0.05$ for comparison to B-6 marrow transplants) and B6-E recipients that were γ irradiated to ablate endogenous innate immune cells ($P < 0.01$ for comparison to B6 marrow transplants). Although the survival rate for the irradiated group was lower than that for the nonirradiated group among mice receiving 129 bone marrow (9/16 surviving [56%] versus 10/13 surviving [77%]), given the number of mice used, this difference in mortality did not reach statistical significance. The overall survival rate was 50% (13/26) in control, infected B6-E mice not given BMT. This survival rate was statistically worse than that for the nonirradiated group receiving 129 BMTs ($P < 0.05$) but not the radiated group, a finding that is consistent with B6-derived innate immune responses being protective. More persuasive of a protective effect of B6 innate cells is the early death and poor overall survival (less than 20%) of wild-

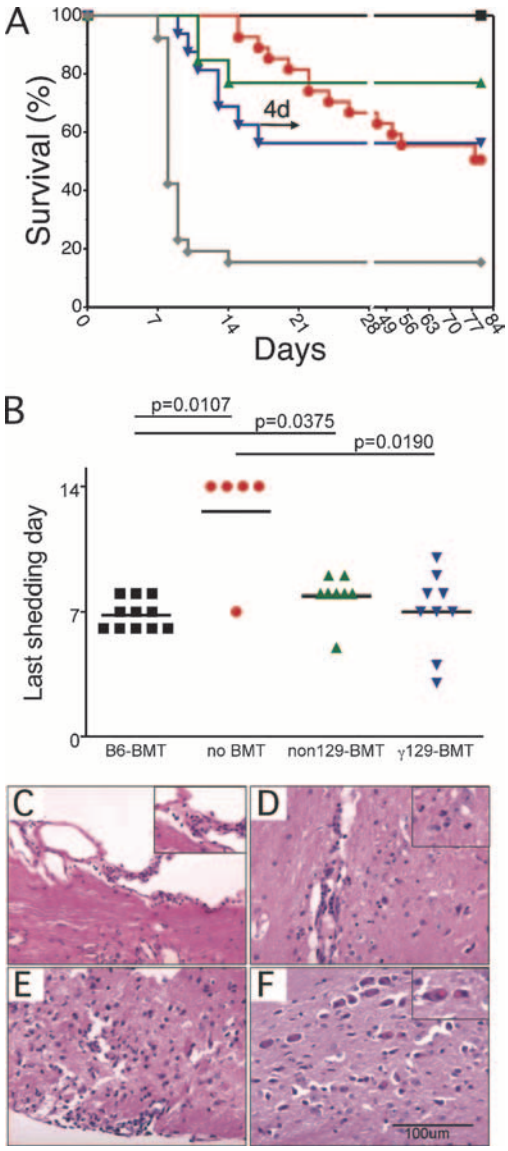

FIG. 5. Transfer of susceptibility and resistance to fatal HSE by BMT. (A) B6-E mice were given no transplant (red circles), given B6 bone marrow (black squares), γ irradiated and given 129 bone marrow (inverted blue triangles), or nonirradiated and given 129 bone marrow (green triangles). Data for 129S6 mice are indicated for comparison (gray diamonds). As indicated by the arrow, 4 days (4d) after the last γ-irradiated mouse receiving 129 BMT died, >80% of non-BMT mice were still alive ($P = 0.026$ [significant]). Mice were infected by corneal scarification with 3,200 PFU HSV-1 17$^+$, and mortality was monitored. Data shown are combined from four experiments. (B) Duration of shedding for individual mice from different groups (as indicated in the figure) is plotted, with mean time of last day of shedding (horizontal line) indicated. Horizontal bars above the graph indicate statistically significant differences between connected groups (representative of two experiments). BS from all four groups of BMT recipients in panel A were examined for pathology associated with HSV infection. Occasional or no viral inclusions were found in neurons in controls receiving no transplant and in recipients of B6 BMT (not shown). The abnormalities found in nonirradiated recipients of 129 BMT were less severe than those in their γ-irradiated counterparts. Shown are sections from γ-irradiated mice receiving 129 BMT. Cellular infiltrates are present in the subarachnoid space (C), perivascular parenchymal infiltrates in the BS (D) (neutrophils are shown in the inset), subpial infiltrating inflammatory cells (E), and prominent viral inclusions in the trigeminal nucleus (F). The inset shows higher magnification of several neurons with nuclear inclusions.

TABLE 2. HSV shedding in tear film from BMT mice during acute infection[a]

Treatment	Day of death	Mouse no.	Result for day:												
			1	2	3	4	5	6	7	8	9	10	11	12	13	14
B6 BMT		A-1	+	+	+	+	−	−	+	+	−	−	−	−	−	−
		A-2	+	+	++	+	+	−	+	−	−	−	−	−	−	−
		A-3	+	+	+	+	−	+	−	−	−	−	−	−	−	−
		A-4	+	+	+	+	+	+	−	−	−	−	−	−	−	−
		A-5	+	+	++	+	+	+	−	−	−	−	−	−	−	−
		A-6	+	+	+	−	+	+	+	−	−	−	−	−	−	−
		A-7	+	+	+	−	−	−	+	−	−	−	−	−	−	−
		A-8	+	+	++	+	+	+	++	+	−	−	−	−	−	−
		A-9	+	+	+	+	−	+	−	−	−	−	−	−	−	−
		A-10	+	+	++	+	−	+	−	−	−	−	−	−	−	−
		A-11	+	+	++	+	+	+	++	+	−	−	−	−	−	−
No BMT	20	B-12	−	+	++	+	+	+	+	+	+	+	+	+	+	+
	24	B-13	−	+	+++	+	+	+	+	+	++	+++	++	++	+++	+
	77	B-14	+	+	++	+	−	+	+	−	−	−	−	−	−	−
		B-15	−	+	+++	+	−	−	++	++	++	+	+	++	+++	+++
		B-16	+	+	+++	+	+	+	+	−	−	+	++	+	+	+
129 BMT		C-17	+	+	+	+	−	−	−	+	−	−	−	−	−	−
		C-18	+	+	+	+	+	+	−	+	−	−	−	−	−	−
		C-19	+	+	++	+	+	−	+	−	+	−	−	−	−	−
		C-20	+	+	++	+	+	−	+	+	−	−	−	−	−	−
		C-21	+	+	+	+	+	−	−	+	+	−	−	−	−	−
		C-22	+	+	+	+	+	−	−	−	−	−	−	−	−	−
		C-23	+	+	+	+	+	−	−	+	−	−	−	−	−	−
	11	C-24	+	+	+	+	+	+	++	+	−	−	−	−	−	−
γ irradiation, 129 BMT[b]		D-25	+	+	+	+	+	+	−	+	−	−	−	−	−	−
	11	D-26	+	+	+	+	+	+	+	+	−	+	−	−	−	−
		D-27	+	+	+	−	−	−	−	−	−	−	−	−	−	−
	17	D-28	+	+	+	+	−	+	+	+	−	−	−	−	−	−
		D-29	+	+	+	−	−	−	+	−	−	−	−	−	−	−
		D-30	−	+	+	+	−	−	−	−	−	−	−	−	−	−
	13	D-31	−	+	+	+	−	+	++	−	−	−	−	−	−	−
		D-32	+	+	+	−	−	+	++	−	−	−	−	−	−	−
	13	D-33	+	+	++	−	+	+	++	−	+	−	−	−	−	−

[a] All mice were swabbed daily until day 14, and the three mice surviving in the no-BMT group were additionally swabbed on days 24 and 39 and determined to be free of virus in the tear film (not shown). Amount of virus in the tear film is indicated as follows: −, no virus detected; +, <10 plaques in swab; ++, 10 to 50 plaques; and +++, >50 plaques. Data shown are from one of two representative experiments.

[b] The recipient was irradiated before BMT.

type 129 mice: more than twice the mortality of B6-E mice, with or without marrow transplant. As further shown in Fig. 5A, mortality of the control nontransplanted B6-E mice was delayed relative to the mice receiving 129 bone marrow, beginning at day 15 p.i. From days 17 through 21 p.i. (Fig. 5A), cumulative mortality was significantly greater among the mice receiving 129 BMTs than among the control B6-E mice not receiving transplants ($P = 0.008$ to 0.026). These results indicate that 129 hematopoietic cells transfer HSE susceptibility, resulting in accelerated mortality compared to the control nontransplanted B6-E mice lacking adaptive immunity.

To determine if the degree of BS inflammation correlated with these mortality results, MRI scans on day 6 p.i. and histopathology studies on day 7 p.i. were carried out with mice receiving transplants. As anticipated, B6-E mice receiving 129 marrow transplants had increased signals on T2 MRI corresponding to the trigeminal root entry zone, similar to what is shown in Fig. 1A, whereas no MRI lesions were detected in B6-E mice receiving B6 marrow transplants (not shown). Similarly, B6-E mice receiving 129 BMTs but not those receiving B6 BMTs had leptomeningeal focal inflammatory cell infiltrates and multiple perivascular and subpial lesions with prominent neutrophils and macrophages (Fig. 5C, D, E, and F). The pathology was most prominent in irradiated B6-E mice receiving 129 BMTs. Only occasional viral inclusion bodies were noted in B6-E mice not receiving transplants, whereas very prominent inclusion bodies in trigeminal neuronal nuclei were seen in B6-E mice receiving 129 BMTs, especially with irradiated 129 bone marrow (not shown).

To determine whether the differences in mortality and inflammation in B6-E mice receiving transplants are also reflected in differences of HSV replication, eye swab cultures were obtained daily after HSV inoculation by the corneal route. As shown in Table 2 and Fig. 5B, there was no significant difference in duration of HSV shedding in B6-E mice receiving either B6 or 129 BMTs (either irradiated or nonirradiated). In contrast, B6-E mice not receiving transplants shed virus for 14 days, 1 week longer then any of the transplant groups. This result is analogous to our prior study showing equivalent necropsy HSV titers in trigeminal ganglia and BS of

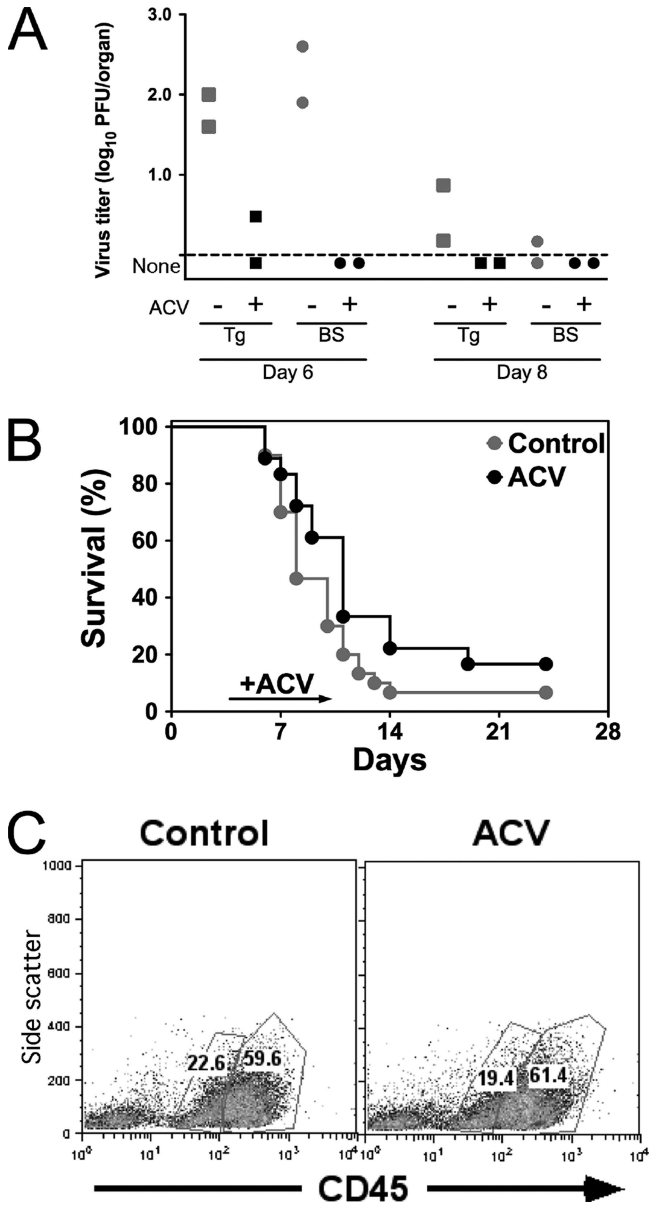

FIG. 6. Effect of ACV on nervous system HSV titer, mortality, and BS inflammation. 129 mice were inoculated with HSV by corneal scarification and given daily i.p. injections with PBS (gray symbols) or 50 mg/kg ACV (black symbols) from day 4 to 10 p.i. (A) HSV titers of trigeminal ganglia (squares) and BS (circles) (data shown are from one of two trials, with two mice in each group sacrificed at days 6 and 8 p.i.); (B) mortality due to HSE (20 control and 14 ACV-treated mice); (C) BS-infiltrating mononuclear cells at day 10 p.i. ($CD45^{high}$ cells are peripheral leukocytes, while $CD45^{int}$ cells are $CD11b^+$ microglia).

susceptible 129 and resistant B6 mice, i.e., HSV titers are not predictive of strain-specific mortality (25).

ACV treatment controls HSV replication but does not prevent BS inflammation and mortality in 129 mice. To support the hypothesis that HSE mortality in this mouse model may be related to bystander inflammation, an attempt was made to separate the effect of viral cytopathology from that of BS inflammation by ACV treatment of HSV-inoculated 129 mice. Timing of treatment was critical in these trials. Virus has been shown to reach the BS by day 3 after corneal inoculation of HSV (44). When ACV treatment was started on day 2 p.i., BS infection, mortality, and BS inflammation were all blocked (not shown). However, as shown in Fig. 6A, ACV initiated on day 4 p.i. reduced viral titers to low or undetectable levels in both trigeminal ganglia and BS homogenates assayed on day 6 p.i. Despite the absence of ongoing HSV replication, mortality in the ACV-treated mice occurred in the usual time course from day 6 to 12 p.i. (Fig. 6B). By day 8 p.i., infectious HSV was no longer detectable in BS of sacrificed control and ACV-treated mice (Fig. 6A). Necropsy BS homogenates of mice in both groups succumbing to the infection on day 9 p.i. and later were negative for infectious HSV, although virus was present in control mice that died earlier (not shown). Even though ACV suppressed HSV BS replication, the BS-inflammatory infiltrates were equivalent in control and ACV-treated mice (Fig. 6C). These results demonstrate that although HSV invasion is required to initiate BS inflammation, the inflammation progresses in the absence of viral replication and mortality correlates with inflammation rather than ongoing viral replication.

DISCUSSION

Our working hypothesis is that tightly regulated innate responses in B6 mice are critical for early restriction of HSV-1 replication. HSV-1 invades the CNS by day 3 p.i. (44), well before the arrival of activated HSV-1-specific T cells, which usually are not detectable until day 8 p.i. (4). While $CD8^+$ T cells have been shown to be proficient at clearing virus late in infection, they do not play a role in limiting spread of virus from peripheral sites of infection to sensory ganglia and the CNS (16, 50). Neurons themselves might also contribute to restriction of HSV-1 replication in the CNS of B6 mice. Notably, the responses of different trigeminal ganglion neurons to HSV-1 infection range from permissive to restrictive, as assessed by antigen and latency-associated transcript expression (27). Additionally, in response to alpha interferon, neurons mount STAT1-dependent responses that reflect the induction of potent innate antiviral mechanisms (52). Consistent with this idea, in a related study we report strong induction of STAT1 expression in trigeminal ganglia of HSV-1-infected 129 mice at day 4 p.i. (24). Local B6-derived CNS innate immunity may also explain the greater resistance of B6-E mice transplanted with 129 bone marrow compared to wild-type 129 mice and also the improved survival of the nonirradiated B6-E mice receiving 129 bone marrow compared to that of the γ-irradiated group receiving 129 bone marrow (Fig. 5).

Although the innate responses in B6 and 129 mice differ, our hypothesis is that the greater inflammatory response in 129 BS (Fig. 1 and 2) results not so much from greater restriction of viral replication in B6 mice as from failure to modulate inflammatory responses in 129 mice. In support of this conclusion is that BS inflammation levels were equivalent in control PBS-treated 129 mice and mice treated with ACV to suppress viral replication (Fig. 6C). ACV in these trials was begun 4 days p.i., just 24 h after HSV reaches the BS from the corneal site of inoculation (44). We speculate that differences in TLR signaling in HSV-infected 129 and B6 mice may result in differences

in activation and chemokine signaling in the brain (2, 20), providing a plausible mechanism to account for the vastly different inflammatory responses observed in the BS.

A number of observations argue in favor of BS inflammation as a major determinant of mortality in this mouse model of HSE. We previously reported increased survival for HSV-inoculated 129 mice treated with MAb to MIG and IP-10 to block CXCR3 signaling, and there was increased survival and decreased BS inflammation in CXCR3 genetically depleted BALB/c mice inoculated with HSV (24). In the present report, we show (i) marked BS inflammation in HSE-susceptible 129 mice compared to that in resistant B6 mice, (ii) enhanced survival in 129 mice depleted of either macrophages or neutrophils, and (iii) an accelerated course of fatal HSE in immunodeficient B6 mice given a 129 bone marrow graft. Consistent with an inflammatory bystander mechanism rather than ongoing viral cytopathology, ACV treatment of 129 mice cleared infectious HSV but did not prevent inflammation or mortality in HSV-inoculated 129 mice (Fig. 6). The prominence of macrophages and neutrophils with a paucity of T cells in the BS inflammatory infiltrate supports a bystander mechanism involving innate cells. Oxidative damage, as indicated by expression of F4-neuroprostanes and F-2 isoprostanes, has been reported in association with neutrophil influx in HSV-infected BALB/c mouse brains (34). This oxidative damage is likely a major mechanism in fatal HSE (30, 49).

The results presented here have important clinical implications for treatment of HSE. Arguments in favor of immune mechanisms in the pathology of fatal HSE have emerged from clinical observations and experimental animal studies (18, 35). HSE occurring during primary infection in neonates may be difficult to diagnose and if not treated promptly is invariably fatal. However, even when diagnosed and treated with high doses of ACV for 21 days, a substantial number of infants with HSE die (3, 36). Moreover, a 2006 study investigating the incidence and pathogenesis of clinical relapse occurring after HSE in adults lends support to immunological mechanisms rather than direct viral cytotoxicity (45). A recent study of HSE in a mouse model with serial cranial MRI reported a significant reduction in the severity of long-term MRI abnormalities in mice treated with ACV in combination with corticosteroids but not in mice treated with ACV or PBS alone (29). Importantly, clinical improvement in abnormal MRI findings was independent of virus load as both groups of ACV-treated mice showed dramatic reductions in virus load in the brain (29). Additionally, it has been reported that corticosteroid treatment does not increase HSV-1 replication and dissemination in a rat model of focal encephalitis (47). However, it was recently reported that the timing of treatment with immunosuppressive steroids is critical (42), consistent with a balanced immune response being required for survival. These results, demonstrating a beneficial effect of combined ACV and corticosteroid therapy over ACV therapy alone, are consistent with host immune responses to HSV-1 being a significant cause of long-term MRI abnormalities in the brain (29, 35, 47). Results from a recent nonrandomized retrospective study using multiple logistic regression analysis identified corticosteroid use as an independent predictor of improved clinical outcome when combined with conventional ACV therapy, indicating the utility of studies conducted with the mouse model (12).

Our data suggest that strategies designed to block or reduce macrophage/microglial and/or neutrophil responses in the CNS of some HSE patients may be beneficial and result in improved survival with reduced morbidity. However, caution is warranted in the application of therapies targeting specific innate cell types, as we have demonstrated that macrophages are protective in the resistant B6 background (26). Ideally, a genetic test for identifying individuals at risk who are susceptible to HSE would facilitate implementation of such targeted immunotherapy, and this may emerge from our studies of genetic resistance to HSE.

ACKNOWLEDGMENTS

We thank Paula V. Welander and Seung-Jae Jung for technical assistance.

This research was supported by grants EY013814 and AI060038 from the National Institutes of Health (National Eye Institute and National Institute of Allergy and Infectious Diseases, respectively).

REFERENCES

1. **Andrews, D. M., V. B. Matthews, L. M. Sammels, A. C. Carrello, and P. C. McMinn.** 1999. The severity of Murray Valley encephalitis in mice is linked to neutrophil infiltration and inducible nitric oxide synthase activity in the central nervous system. J. Virol. **73:**8781–8790.
2. **Aravalli, R. N., S. Hu, T. N. Rowen, J. M. Palmquist, and J. R. Lokensgard.** 2005. Cutting edge: TLR2-mediated proinflammatory cytokine and chemokine production by microglial cells in response to herpes simplex virus. J. Immunol. **175:**4189–4193.
3. **Bale, J. F., and L. J. Miner.** 2005. Herpes simplex virus infections of the newborn. Curr. Treat. Options Neurol. **7:**151–156.
4. **Cantin, E. M., D. R. Hinton, J. Chen, and H. Openshaw.** 1995. Gamma interferon expression during acute and latent nervous system infection by herpes simplex virus type 1. J. Virol. **69:**4898–4905.
5. **Chen, S.-H., H.-W. Yao, W.-Y. Huang, K.-S. Hsu, H.-Y. Lei, A.-L. Shiau, and S.-H. Chen.** 2006. Efficient reactivation of latent herpes simplex virus from mouse central nervous system tissues. J. Virol. **80:**12387–12392.
6. **Ciavarra, R. P., L. Taylor, A. R. Greene, N. Yousefieh, D. Horeth, N. van Rooijen, C. Steel, B. Gregory, M. Birkenbach, and M. Sekellick.** 2005. Impact of macrophage and dendritic cell subset elimination on antiviral immunity, viral clearance and production of type 1 interferon. Virology **342:**177–189.
7. **Fleming, T. J., M. L. Fleming, and T. R. Malek.** 1993. Selective expression of Ly-6G on myeloid lineage cells in mouse bone marrow. RB6-8C5 mAb to granulocyte-differentiation antigen (Gr-1) detects members of the Ly-6 family. J. Immunol. **151:**2399–2408.
8. **Ford, A. L., A. L. Goodsall, W. F. Hickey, and J. D. Sedgwick.** 1995. Normal adult ramified microglia separated from other central nervous system macrophages by flow cytometric sorting. Phenotypic differences defined and direct ex vivo antigen presentation to myelin basic protein-reactive CD4+ T cells compared. J. Immunol. **154:**4309–4321.
9. **Fry, T. J., and C. L. Mackall.** 2001. Interleukin-7: master regulator of peripheral T-cell homeostasis? Trends Immunol. **22:**564–571.
10. **Hesslein, D. G. T., S. Y. Yang, and D. G. Schatz.** 2006. Origins of peripheral B cells in IL-7 receptor-deficient mice. Mol. Immunol. **43:**326–334.
11. **Ismail, H. F., P. Fick, J. Zhang, R. G. Lynch, and D. J. Berg.** 2003. Depletion of neutrophils in IL-10-/- mice delays clearance of gastric Helicobacter infection and decreases the Th1 immune response to Helicobacter. J. Immunol. **170:**3782–3789.
12. **Kamei, S., T. Sekizawa, H. Shiota, T. Mizutani, Y. Itoyama, T. Takasu, T. Morishima, and K. Hirayanagi.** 2005. Evaluation of combination therapy using aciclovir and corticosteroid in adult patients with herpes simplex virus encephalitis. J. Neurol. Neurosurg. Psychiatry **76:**1544–1549.
13. **Kang, J., M. Coles, and D. H. Raulet.** 1999. Defective development of gamma/delta T cells in interleukin 7 receptor-deficient mice is due to impaired expression of T cell receptor gamma genes. J. Exp. Med. **190:**973–982.
14. **Krakowski, M. L., and T. Owens.** 1997. The central nervous system environment controls effector CD4+ T cell cytokine profile in experimental allergic encephalomyelitis. Eur. J. Immunol. **27:**2840–2847.
15. **Kramnik, I., and V. Boyartchuk.** 2002. Immunity to intracellular pathogens as a complex genetic trait. Curr. Opin. Microbiol. **5:**111–117.
16. **Lang, A., and J. Nikolich-Zugich.** 2005. Development and migration of protective CD8+ T cells into the nervous system following ocular herpes simplex virus-1 infection. J. Immunol. **174:**2919–2925.
17. **Lantz, C. S., J. Boesiger, C. H. Song, N. Mach, T. Kobayashi, R. C. Mulligan, Y. Nawa, G. Dranoff, and S. J. Galli.** 1998. Role for interleukin-3 in mast-cell and basophil development and in immunity to parasites. Nature **392:**90–93.

18. **Lellouch-Tubiana, A., M. Fohlen, O. Robain, and F. Rozenberg.** 2000. Immunocytochemical characterization of long-term persistent immune activation in human brain after herpes simplex encephalitis. Neuropathol. Appl. Neurobiol. **26:**285–294.
19. **Lokensgard, J. R., M. C. Cheeran, S. Hu, G. Gekker, and P. K. Peterson.** 2002. Glial cell responses to herpesvirus infections: role in defense and immunopathogenesis. J. Infect. Dis. **186**(Suppl. 2)**:**S171–S179.
20. **Lokensgard, J. R., S. Hu, W. Sheng, M. vanOijen, D. Cox, M. C. Cheeran, and P. K. Peterson.** 2001. Robust expression of TNF-alpha, IL-1beta, RANTES, and IP-10 by human microglial cells during nonproductive infection with herpes simplex virus. J. Neurovirol. **7:**208–219.
21. **Lopez, C.** 1975. Genetics of natural resistance to herpesvirus infections in mice. Nature **258:**152–153.
22. **Lopez, C.** 1981. Resistance to herpes simplex virus—type 1 (HSV-1). Curr. Top. Microbiol. Immunol. **92:**15–24.
23. **Lopez, C.** 1980. Resistance to HSV-1 in the mouse is governed by two major, independently segregating, non-H-2 loci. Immunogenetics **11:**87–92.
24. **Lundberg, P., H. Openshaw, M. Wang, H. J. Yang, and E. Cantin.** 2007. Effects of CXCR3 signaling on development of fatal encephalitis and corneal and periocular skin disease in HSV-infected mice are mouse-strain dependent. Investig. Ophthalmol. Vis. Sci. **48:**4162–4170.
25. **Lundberg, P., P. Welander, H. Openshaw, C. Nalbandian, C. Edwards, L. Moldawer, and E. Cantin.** 2003. A locus on mouse chromosome 6 that determines resistance to herpes simplex virus also influences reactivation, while an unlinked locus augments resistance of female mice. J. Virol. **77:**11661–11673.
26. **Lundberg, P., P. V. Welander, C. K. Edwards III, N. van Rooijen, and E. Cantin.** 2007. Tumor necrosis factor (TNF) protects resistant C57BL/6 mice against herpes simplex virus-induced encephalitis independently of signaling via TNF receptor 1 or 2. J. Virol. **81:**1451–1460.
27. **Margolis, T. P., F. Sedarati, A. T. Dobson, L. T. Feldman, and J. G. Stevens.** 1992. Pathways of viral gene expression during acute neuronal infection with HSV-1. Virology **189:**150–160.
28. **Metcalfe, D. D., D. Baram, and Y. A. Mekori.** 1997. Mast cells. Physiol. Rev. **77:**1033–1079.
29. **Meyding-Lamade, U. K., C. Oberlinner, P. R. Rau, S. Seyfer, S. Heiland, J. Sellner, B. T. Wildemann, and W. R. Lamade.** 2003. Experimental herpes simplex virus encephalitis: a combination therapy of acyclovir and glucocorticoids reduces long-term magnetic resonance imaging abnormalities. J. Neurovirol. **9:**118–125.
30. **Milatovic, D., Y. Zhang, S. J. Olson, K. S. Montine, L. J. Roberts II, J. D. Morrow, T. J. Montine, T. S. Dermody, and T. Valyi-Nagy.** 2002. Herpes simplex virus type 1 encephalitis is associated with elevated levels of F2-isoprostanes and F4-neuroprostanes. J. Neurovirol. **8:**295–305.
31. **Miller, C. L., V. I. Rebel, C. D. Helgason, P. M. Lansdorp, and C. J. Eaves.** 1997. Impaired steel factor responsiveness differentially affects the detection and long-term maintenance of fetal liver hematopoietic stem cells in vivo. Blood **89:**1214–1223.
32. **Naito, M., S. Umeda, T. Yamamoto, H. Moriyama, H. Umezu, G. Hasegawa, H. Usuda, L. D. Shultz, and K. Takahashi.** 1996. Development, differentiation, and phenotypic heterogeneity of murine tissue macrophages. J. Leukoc. Biol. **59:**133–138.
33. **Niemialtowski, M. G., and B. T. Rouse.** 1992. Predominance of Th1 cells in ocular tissues during herpetic stromal keratitis. J. Immunol. **149:**3035–3039.
34. **Nocka, K., J. C. Tan, E. Chiu, T. Y. Chu, P. Ray, P. Traktman, and P. Besmer.** 1990. Molecular bases of dominant negative and loss of function mutations at the murine c-kit/white spotting locus: W37, Wv, W41 and W. EMBO J. **9:**1805–1813.
35. **Openshaw, H., and E. M. Cantin.** 2005. Corticosteroids in herpes simplex virus encephalitis. J. Neurol. Neurosurg. Psychiatry **76:**1469.
36. **O'Riordan, D. P., W. C. Golden, and S. W. Aucott.** 2006. Herpes simplex virus infections in preterm infants. Pediatrics **118:**e1612–e1620.
37. **Peschon, J. J., P. J. Morrissey, K. H. Grabstein, F. J. Ramsdell, E. Maraskovsky, B. C. Gliniak, L. S. Park, S. F. Ziegler, D. E. Williams, C. B. Ware, et al.** 1994. Early lymphocyte expansion is severely impaired in interleukin 7 receptor-deficient mice. J. Exp. Med. **180:**1955–1960.
38. **Reith, A. D., R. Rottapel, E. Giddens, C. Brady, L. Forrester, and A. Bernstein.** 1990. W mutant mice with mild or severe developmental defects contain distinct point mutations in the kinase domain of the c-kit receptor. Genes Dev. **4:**390–400.
39. **Roizman, B., and A. E. Sears.** 1987. An inquiry into the mechanisms of herpes simplex virus latency. Annu. Rev. Microbiol. **41:**543–577.
40. **Roos, K. L.** 1999. Encephalitis. Neurol. Clin. **17:**813–833.
41. **Segal, S., and A. V. Hill.** 2003. Genetic susceptibility to infectious disease. Trends Microbiol. **11:**445–448.
42. **Sergerie, Y., G. Boivin, D. Gosselin, and S. Rivest.** 2007. Delayed but not early glucocorticoid treatment protects the host during experimental herpes simplex virus encephalitis in mice. J. Infect. Dis. **195:**817–825.
43. **Sergerie, Y., S. Rivest, and G. Boivin.** 2007. Tumor necrosis factor-alpha and interleukin 1-beta play a critical role in the resistance against lethal herpes simplex virus encephalitis. J. Infect. Dis. **196:**853–860.
44. **Shimeld, C., S. Efstathiou, and T. Hill.** 2001. Tracking the spread of a *lacZ*-tagged herpes simplex virus type 1 between the eye and the nervous system of the mouse: comparison of primary and recurrent infection. J. Virol. **75:**5252–5262.
45. **Sköldenberg, B., E. Aurelius, A. Hjalmarsson, F. Sabri, M. Forsgren, B. Andersson, A. Linde, Ö. Strannegård, M. Studahl, L. Hagberg, and L. Rosengren.** 2006. Incidence and pathogenesis of clinical relapse after herpes simplex encephalitis in adults. J. Neurol. **253:**163–170.
46. **Thomas, J., S. Gangappa, S. Kanangat, and B. T. Rouse.** 1997. On the essential involvement of neutrophils in the immunopathologic disease: herpetic stromal keratitis. J. Immunol. **158:**1383–1391.
47. **Thompson, K. A., W. W. Blessing, and S. L. Wesselingh.** 2000. Herpes simplex replication and dissemination is not increased by corticosteroid treatment in a rat model of focal Herpes encephalitis. J. Neurovirol. **6:**25–32.
48. **Tumpey, T. M., S. H. Chen, J. E. Oakes, and R. N. Lausch.** 1996. Neutrophil-mediated suppression of virus replication after herpes simplex virus type 1 infection of the murine cornea. J. Virol. **70:**898–904.
49. **Valyi-Nagy, T., S. J. Olson, K. Valyi-Nagy, T. J. Montine, and T. S. Dermody.** 2000. Herpes simplex virus type 1 latency in the murine nervous system is associated with oxidative damage to neurons. Virology **278:**309–321.
50. **van Lint, A., M. Ayers, A. G. Brooks, R. M. Coles, W. R. Heath, and F. R. Carbone.** 2004. Herpes simplex virus-specific CD8+ T cells can clear established lytic infections from skin and nerves and can partially limit the early spread of virus after cutaneous inoculation. J. Immunol. **172:**392–397.
51. **Van Rooijen, N., and A. Sanders.** 1994. Liposome mediated depletion of macrophages: mechanism of action, preparation of liposomes and applications. J. Immunol. Methods **174:**83–93.
52. **Wang, J., and I. L. Campbell.** 2005. Innate STAT1-dependent genomic response of neurons to the antiviral cytokine alpha interferon. J. Virol. **79:**8295–8302.
53. **Waskow, C., S. Paul, C. Haller, M. Gassmann, and H. Rodewald.** 2002. Viable c-Kit(W/W) mutants reveal pivotal role for c-kit in the maintenance of lymphopoiesis. Immunity **17:**277–288.
54. **Whitley, R. J.** 2002. Herpes simplex virus infection. **13:**6–11.
55. **Whitley, R. J., and J. W. Gnann.** 2002. Viral encephalitis: familiar infections and emerging pathogens. Lancet **359:**507–513.
56. **Whitley, R. J., D. W. Kimberlin, and B. Roizman.** 1998. Herpes simplex viruses. Clin. Infect. Dis. **26:**541–555.
57. **Zhou, J., S. A. Stohlman, D. R. Hinton, and N. W. Marten.** 2003. Neutrophils promote mononuclear cell infiltration during viral-induced encephalitis. J. Immunol. **170:**3331–3336.